Active Distribution Network Operation: A Market-based Approach

Rana H.A. Zubo and Geev Mokryani, *Senior Member, IEEE*

***Abstract*— This paper proposes a novel technique for operation of distribution networks with considering active network management (ANM) schemes and demand response (DR) within a joint active and reactive distribution market environment. The objective of proposed model is to maximize social welfare using market-based joint active and reactive optimal power flow (OPF). Firstly, the intermittent behavior of renewable sources (solar irradiance, wind speed) and load demands is modeled through Scenario-Tree technique. Then, a network frame is recast using mixed-integer linear programming (MILP), which is solvable using efficient off-the-shelf branch-and cut solvers. Additionaly, this work explores the impact of wind and solar power penetration on the active and reactive distribution locational prices (D-LMPs) within the distribution market environment with integration of ANM schemes and DR. A realistic case study (16-bus UK generic medium voltage distribution system) is used to demonstrate the effectiveness of the proposed method.**

***Index Terms*-Active network management, demand response, uncertainty modeling, joint active/reactive distribution electricity market, social welfare maximization, distribution locational marginal prices and mixed- integer linear programming.**

a) Index and Sets

i,j	Index of buses
ss	Index of substation
l	Index of loads
w	Index of wind turbine
pv	Index of photovoltaic units (PVs)
s	Index for scenarios

b) Parameter

$C_i^{l,P}$	Active power bid prices for load at bus *i*
$C_i^{l,Q}$	Reactive power bid prices for load at bus *i*
$C_i^{DR,P}$	Active power bid prices for demand response at bus *i*
$C_i^{DR,Q}$	Reactive power bid prices for demand response at bus *i*
$C_i^{ss,P}$	Substation active power offer prices at bus *i*
$C_i^{ss,Q}$	Substation reactive power offer prices at bus *i*
$C_i^{w,P}$	WTs active power offer prices at bus *i*
$C_i^{PV,P}$	PVs active power offer prices at bus *i*
$P_{i,s}^{l,\min}, P_{i,s}^{l,\max}$	Minimum and maximum active power for load at bus *i* at scenario *s*
$P_{i,s}^{DR,\min}, P_{i,s}^{DR,\max}$	Minimum and maximum active power for demand response at bus *i* at scenario *s*
$Q_i^{ss,\min}, Q_i^{ss,\max}$	Minimum and maximum reactive power for substation at bus *i*
$Q_{i,s}^{w,\min}, Q_{i,s}^{w,\max}$	Minimum and maximum reactive power for WTs at bus *i* at scenario *s*
$Q_{i,s}^{PV,\min}, Q_{i,s}^{PV,\max}$	Minimum and maximum reactive power for PVs at bus *i* at scenario *s*
$Q_{i,s}^{l,\min}, Q_{i,s}^{l,\max}$	Minimum and maximum reactive power for loads at bus *i* at scenario *s*
$Q_{i,s}^{DR,\min}, Q_{i,s}^{DR,\max}$	Minimum and maximum reactive power for demand response at bus *i* at scenario *s*
$P_{i,j}^{+}, P_{i,j}^{-}$	active power flow in i,j in the forward/ backward direction
$Q_{i,j,s}^{+}, Q_{i,j,s}^{-}$	reactive power flow in i,j in the forward/ backward direction
$T_{i,j}^{\min} / T_{i,j}^{\max}$	Minimum and Maximum of tap ratio in the OLTC
$I^{\max}$	Maximum current flow of conductors
$R_{i,j}, X_{i,j}, Z_{i,j}$	Resistance and Reactance magnitude and impedance of conductors respectively (Ω/km)
R^{tot}	Total number of block in the piecewise linearization
Vc/*I*c	Converter voltage/current
V_t	Connection point grid voltage
$\Delta S_{i,j}$	Upper bound of each block of the power flow of branch *i,j*
$m_{i,j}$	Slope of the rth block of the power flow of the branch *i,j*
Q_{mnd}	Mandatory reactive power of PVs and WTs
Q^{min}	Minimum reactive power of PVs and WTs
Q^{max}	Maximum reactive power of PVs and WTs
Q_{av}	Maximum availability reactive power of PVs and WTs
m_1	Offered cost of losses of RDGs
m_2	Offered opportunity cost of RDGs
$QPF_i^{w,pv}$	WTs and PVs reactive power offer prices at bus *i*

c) Variables

$P_{i,s}^{l}$	Active power for load at bus *i* at scenario *s*
$P_{i,s}^{ss}$	Active power for substation at bus *i* at scenario *s*
$P_{i,s}^{w}$	Active power for WTs at bus *i* at scenario *s*
$P_{i,s}^{PV}$	Active power for PVs at bus *i* at scenario *s*
$P_{i,s}^{DR}$	Active power for demand response at bus *i* at scenario *s*
$Q_{i,s}^{l}$	Reactive power for loads at bus *i* at scenario *s*
$Q_{i,s}^{ss}$	Reactive power for substation at bus *i* at scenario s
$Q_{i,s}^{w}$	WTs reactive power at bus *i* at scenario *s*
$Q_{i,s}^{PV}$	PVs reactive power at bus *i* at scenario s
$Q_{i,s}^{DR}$	Reactive power for demand response at bus *i* at scenario *s*
$T_{i,j}$	Tap setting in the OLTC
V_i^{sq}, V_j^{sq}	Square of voltage magnitude
$I_{i,j}^{sq}$	Square of current magnitude
$y_{i,j,s}$	Binary variable of feeder section
$S_{i,j}$	Apparent power flow
$V_i^{\min} / V_i^{\max}$	Min/Max values of the voltage at bus *i*.
$V_{i,s}$	Instantaneous voltage at bus *i* and scenario *s*.
u_{ij}	Binary utilization variable for all feeders (substation, WTs and PV).
π_s	Probabilities of demand load, solar irradiance, and the active offer prices of PV and WTs

I. Introduction

A. Background and Motivation

Integration of renewable distributed generators (RDGs) (e.g. photovoltaic cells (PVs) and wind turbines (WTs)) have been considered as one of the issues for the power distribution system [1]. The intermittent generation of PVs and WTs introduce both technical and commercial challenges which include, voltage stability, voltage violation and power losses to distribution network operators (DNOs) [2]. Addressing these challenges, the DNOs need to consider the development of new methodologies and models to deal with the uncertainty associated with WTs and PVs [3, 4]. Active network management (ANM) schemes at distribution level including coordinated voltage control (CVC) of on-load tap changers (OLTCs) and adaptive power factor control (PFC) offer a feasible solution for DNOs for optimal operation for network assets with a high penetration of RDGs at the same time considering uncertainties related to output power of WTs and PVs, market constraints, and power flows schedule with the interface to the transmission system [5, 6]. ANM seek to decrease the deviation in voltage and power losses and reactive power compensators [7]. In general, ANM can be defined as smart control techniques based on real time measurement of voltage and current which provides benefits in facilitating the increasing integration of RDGs [8].

Demand response (DR) is another additional option, which provide economic reliability benefits and mitigate the impact of RDGs uncertainties. DR is defined as the ability of consumers to change their consumption behavior patterns of electricity in order to improve the reliability of system [9].

Under the decentralized electric power systems scheme, at all times, the boundaries of frequency and voltage limits must be sustained within a specified limit in order to fullfil the required safety and security standards.

In order to solve this problem, a set of special services are required to ensure a stable and safe operation of the electric supply [10]. These are known as ancillary services because they complement the energy product and provide open access transmission, supply reactive demand, control system voltage and support system security [11]. One of the primary objectives of DNOs is to provide these ancillary services which are classified as active power services which deal with load frequency regulation, and reactive power services which include voltage control [11, 12]. Usually, the voltage instability in the power network is due to non existence of reactive power ancillary services, which may lead to the collapse of the power system and this is the main reason for the power outage [13].

B. Literature review and Research gap

Previous research has focused on the active power ancillary services at the transmission level. For instance, in [14] two new frequency control constraints are introduced namely, the minimum frequency constraint, and the rate of change of frequency constraint and are illustrated how these constraints can be included in a market dispatch formulation are introduced. A new market model for implementation a primary frequency response of ancillary service into pool-based restructured power markets is proposed in [15], a day-ahead energy market which includes a primary frequency reserve from generators and fast frequency response reserve from load resources is introduced [16].

Other studies have addressed the mitigation of the impact of reactive ancillary services in transmission systems. Reference [17] has proposed a day-ahead market for reactive power based on pay-as-bid pricing mechanism in the transmission system considering the reactive power behavior during the market clearing period, and multi-objective optimization technique based on reactive power market clearing which consider voltage stability is presented [18, 19].

A new stochastic model based on the decoupled day-ahead active and reactive power markets at distribution level has been proposed with considering active network management (ANM) schemes in order to scheduling the active and reactive power in distribution system with RDGs [20], the reactive power market settlement procedure for DGs in distribution network for reactive power ancillary services which minimize the DNOs reactive power payment and enhance the voltage profile for DGs [21], another model is the combination of ANM with DR program to minimize the costs which are beneficial to both economy and environment [22].

Therefore, establishing a joint active and reactive power market at distribution level is considered to be a successful technique for efficiently managing and hosting a large amount of RDGs in distribution networks [23].

However, none of the literature studies introduced the joint active and reactive power market model at the distribution level and assessed the impact of active and reactive power on the amount of active and reactive power that can be injected/absorbed to/from the grid from WTs and PV with integration of ANM schemes and DR program. The gap that this paper tries to fill is to investigate the impact of DR and ANM schemes on active and reactive power generated by RDGs within a novel electricity market.

Table1 is a summary of all the references and differences between them and the state of the art.

TABLE 1
COMPARISON OF EXISTING LITERATURE WITH PRPOSED MODEL

Reference	Transmission or distribution level	Renew able -energy	Correlation	DR	Power market		ANM	SW Max.
					active	reactive		
[14-16]	Transmission	✓	×	×	✓	×	×	×
[17-19]	Transmission	×	×	×	×	✓	×	×
[20]	Distribution	✓	×	×	✓	✓	✓	×
[21]	Distribution	✓	×	×	×	✓	×	×
[22]	Distribution	✓	×	✓	✓	×	✓	×
Proposed	**Distribution**	✓	✓	✓	✓	✓	✓	✓

C. Aims and contributions

The main aim of this paper is to maximize SW using market-based active and reactive OPF considering ANM schemes and DR programs. In addition, the impact of wind and solar power penetration on the SW and on active and reactive D-LMPs is investigated.

The voltage and reactive power control can be an alternative to the increase of the participation of the DGs in the distribution networks, since the active and reactive power management can be smartly coordinated by external control in order to eliminate both under voltage and over voltage violations in the distribution networks [24]. In order to achieve an optimum voltage profile over the distribution feeders and optimum reactive power flows in the system, Active Network

Management (ANM) including on load tap changer (OLTC) transformers, DGs power factor control and demand response can play an important role to decrease the deviation in voltage and reactive power compensators [25].

On the other hand, the electrical distribution system became more active to comply with the connection of large amount of DGs. Demand response (DR) program is an attractive way to address this issue as it can respond quickly with respect to the variation of DGs [26].

Integration of ANM and DR in the distribution system creates opportunities to more efficiently balance supply and demand [27]. In addition, they are a key means for the smooth incorporation of RDGs into power systems, and it considers distribution system operators (DSOs) as the agents for integration of RDGs into the electricity market that can maximize the share of renewable energy system in overall energy consumption[28]. Also, with ANM schemes, DNOs will be capable of optimizing use of their assets by dispatching generation, controlling OLTCs and voltage regulators and managing reactive power [29]

This paper proposes a joint active and reactive optimal power flow in order to evaluate the amount of active and reactive power that can be injected/absorbed to/from the grid from WTs and PVs is proposed to offer a means of measuring the impact of ANM schemes and DR programs on connectable active and reactive power capacity which generated by wind and PVs. In addition, to effectively handling the time-variation of multiple renewable sites and demand, it also considers ANM to allow maximum absorption of WTs and PVs generation capacity while respecting voltage statutory limits and thermal constraints. ANM schemes including coordinated voltage control (CVC) of on-load tap changers (OLTCs) are embedded within the formulation.

Another innovative contribution of the proposed method, the contribution of DNOs in a joint active/reactive distribution market including a day-ahead and a real-time intraday schedule of WTs, PVs and load demand according to the market price is evaluated. The implementation of a distribution-level market based on active and reactive D-LMPs provides opportunities for real-time pricing that necessitates the implementation of innovative technologies, such as smart grids [21].

Mixed- integer linear optimization program (MILP) is used to clear the proposed joint active and reactive distribution market. MILP is applied because: 1) the mathematical model is robust; 2) the computational behavior of a linear solver is more efficient than nonlinear ones; and 3) using classical optimization techniques, convergence can be guaranteed. The steady-state operation of a radial electrical distribution network is complicated to model linearly hence, an alternative current (ac) flow is approximated through linear expressions.

Non-linear technique has several drawbacks, including slow convergence, complexity, and difficulties involved in handling constraint and in adapting to different problem. In addition, it is non-convex therefore finding a global solution for problem is challenging.

In this paper the proposed nonlinear model is converted to MILP model. Owing to the convexity, the proposed model can guarantee convergence of optimality and can be solved efficiently with commercial solver. Also linearization technique is very convenient for handling the constraints, providing global optimal solution.

This paper proposes a stochastic method to assess the amount of wind and solar power peneteration on the social welfare (SW) and on active and reactive distribution location marginal prices (D-LMP) within a novel distribution market model taking into account the uncertainties related to wind speed, solar irradiance and load demand with integration of ANM and DR.

The main contributions of this paper are highlighted as follows:

- To design a joint active and reactive electricity market model at distribution level with active ANM schemes and demand response (DR) within.
- To introduce a novel formulation for optimal operation of distribution networks within a proposed joint active and reactive distribution with the integration of ANM schemes and DR using mixed-integer linear programming (MILP).
- Modeling the correlation between the uncertainties associated with load demand and power generated by WTs and PVs, abovementioned uncertainties using Scenario-Tree approach.

D. Paper organization

The rest of this paper is structured as follows: Uncertainty modeling is presented in Section II, distribution market model and formulation in Section III, illustration of a case study in section IV, simulation results in case V and finally the conclution in section VI.

II. UNCERTAINTY MODELLING

A. Wind speed modelling

In this study, Weibull probability density function (PDF) is used to model the variation of wind speed [30]. The PDF function which relates the wind speed and the output power of WTs is given by [31] as follows:

$$PDF(v) = (\frac{k}{c})(\frac{v}{c})^{k-1} \exp\left[-(\frac{v}{c})^{k}\right] \quad (1)$$

where v, k, and c are wind speed, shape index, and the scale index of the Weibull PDF of wind speed respectively.

The relationship between the wind speed v and the output power of WTs P_w can be determined using operational parametere (rated power output P_{rated} (kW), cut-off wind speed v_{co} (m/s), cut-in wind speed v_{ci} (m/s), and rated wind speed v_r (m/s)). According to the speed power curve of WTs, the generated power of WTs is represented as follows [32-34]:

$$P_w(v) = \begin{cases} 0, & 0 \le v \le v_{ci} \\ P_{rated} \times \dfrac{v - v_{ci}}{v_r - v_{ci}}, & v_{ci} \le v \le v_r \\ P_{rated}, & v_r \le v \le v_{co} \\ 0, & v_{co} \le v \end{cases} \quad (2)$$

Therefore, the WTs active power output at bus i and scenario s can be defined as follows:

$$0 \le P^{w}_{i,s} \le \gamma^{w}_{i,s} \times P^{w}_{i,rated} \quad (3)$$

where $\gamma^{w}_{i,s}$ is the percentage of WTs active and reactive power output at scenario s.

B. Solar irradiance modelling

Beta PDF is used to model solar irradiance which is given by the following equation:

$$PDF(s)=\begin{Bmatrix}\frac{\Gamma(\alpha+\beta)}{\Gamma(\alpha)+\Gamma(\beta)}\times s^{\alpha-1}\times(1-s)^{\beta-1}, & 0\le s\le 1, 0\le \alpha,\beta\\ 0 & else\end{Bmatrix} \quad (4)$$

where s represents the solar irradiance (kW/m^2). α and β can be obtained as follows:

$$\alpha=\frac{\mu\times\beta}{1-\mu} \quad (5)$$

$$\beta=(1-\mu)\times\left(\frac{\mu\times(1-\mu)}{\sigma^2}-1\right) \quad (6)$$

where μ is mean value and σ is the standard deviation of the random variable. To estimate the cell temperature, the solar irradiance, and the output power of PVs, Eqs. (7) and (8) are used [35]:

$$P_{pv}=P_{STC}\left\{\frac{G}{1000}\left[1+\delta\left(T_{cell}-25\right)\right]\right\} \quad (7)$$

$$T_{cell}=T_{amb}+\left(\frac{NOCT-20}{800}\right)G \quad (8)$$

where P_{pv}, P_{STC} are the output power and the power under standard test condition in (W) respectively. δ is the power-temperature coefficient in (%/°C), T_{cell}, T_{amb} and $NOCT$ are the cell temperature in °C, the ambient temperature in °C, and normal operating cell temperature conditions in °C, respectively. G is solar irradiance in (W/m^2).

C. Load demand modelling

For each bus, load demand is modelled using Gaussian PDF. The PDF for load l is calculated as follows [36, 37]:

$$PDF(l)=\frac{1}{\sigma_l\sqrt{2\pi}}\times\exp\left[-\left(\frac{\left(l-\mu_l\right)^2}{2{\sigma_l}^2}\right)\right] \quad (9)$$

where μ_l is mean value and σ_l is standard deviation.

D. Modeling approach

The scenario tree techniques have been widely used in the framework of stochastic programming methods to deal with decision making problem under uncertainty. Instead of giving a point estimation of multivariate random variables scenario tree approach provides likely scenarios of future with associated probabilities. The scenarios can cover only the next time step or even more steps ahead in time.

To model the uncertainty and correlation of the load demand, wind speed, and solar irradiation, duration curves for each one are presented. All load demand, wind speed, and solar irradiation are jointly modelled as described below.

Historical data for 8760 hours of the year is categorized into different categories including load demand, solar irradiance and wind speed so that we can get factorized data. The obtained data is employed to construct load demand curve and the data is also organized from maximum to minimum values, while keeping the correlation among various hourly data of solar irradiation, wind speed and load demand, as shown in Fig. 1. The time slots are placed to regulate load duration curve, and its length is changing along the load duration. For each time slot, the historical data of load demand, wind speed and solar irradiance are organized in descending order in order to consider carefully the load demand in this model. The cumulative distribution function for each block of the load demand, solar irradiance and wind speed are determined. Each cumulative distribution function is split into a number of segments with their corresponding related to probability (i.e. the demand level that can be obtained in every time slot). The scenarios are defined by combination of the levels of uncertain data for each time block. Thus, for every load level *ll*, each scenario *s* comprises the maximum level of power supply by PV sell $\mu^{\theta}_{ll,s}$, a maximum level of power generated by WTs $\mu^{w}_{ll,s}$ and an average demand factor $\mu^{D}_{ll,s}$.The total number of scenarios is 108 (four-time blocks, three load demand levels, three solar irradiation levels and three wind speed levels (4×3×3×3=108)).

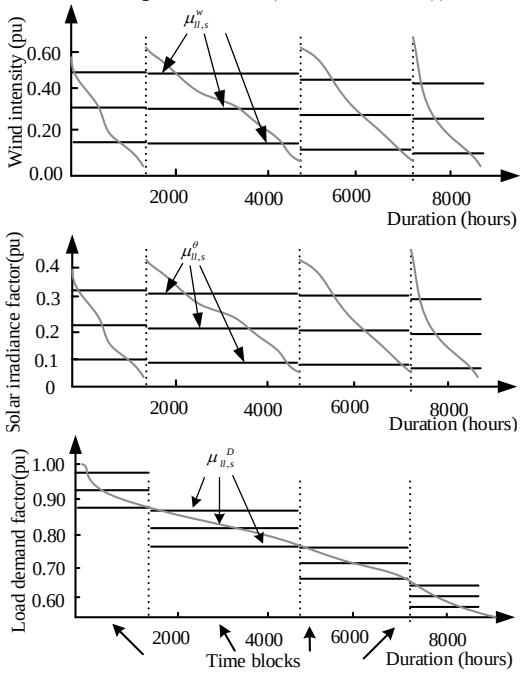

Fig.1. Load demand, wind speed, solar irradiance curves and level

III. DISTRIBUTION MARKET MODEL

In this section, a novel joint active and reactive market model is proposed at distribution level. The formulation of the suggested model within DNOs control area is based on bilateral contracts and a pooling as depicted in Fig. 2. The DNO serves as distribution market operator, where it is handling and contributing to the operational supplies such as purchasing the active and reactive power via bilateral contracts. Every hour, the dispatchable load demands, wind turbines and photovoltaics submit their active and reactive power offers to the distribution market in the form of blocks. The DNO's aim is to clear the market by maximizing the SW using the joint active and reactive OPF subject to network constraints.

The following actions are taken by the proposed distribution market:

1) A day-ahead schedule is formed for dispatchable loads, wind turbines and photovoltaics, based on market prices. On each trading day, dispatchable loads, wind turbines and

photovoltaics dispatch both their offers , a day before the trading duration [21].

2) Adjustment market, which closes a few hours prior to delivery to make correction happened due to unplanned supply and demand variations during that period because of load and demand imbalance.
3) Intra-day operational optimization in real-time is done for the sake of profitability by altering the schedule every 15 minutes (balancing market).

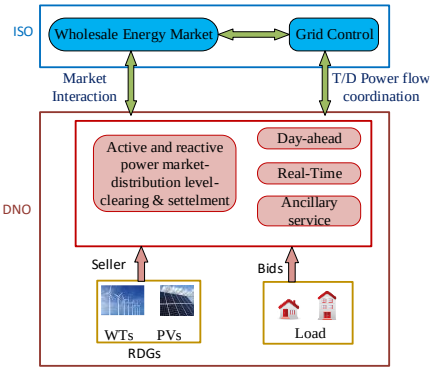

Fig.2.The structure of the proposed distribution market

In the day-ahead market, in order to eliminate or minimize the imbalance between the quantity of energy cleared and the anticipated production, the operations are taken in the adjustment and in real-time distribution markets are needed. In the adjustment market, wind turbines and photovoltaics are allowed to revise their approximated production in their offers, which helps decrease the associated uncertainties. The real-time variations between the supply and demand is fixed by balancing market to make sure that the supply and demand balance.

The market clearing price and quantity are calculated by maximizing SW while taking into account the network constraints with incorporation of DR and ANM schemes integration within the proposed distribution market.

In this paper, mixed-integer non-linear programming MINLP model is converted to MILP model by utilizing a very precise linearization method. The proposed MILP model can be solved utilizing a standard off-the shelf mathematical programming solvers, which offers ensured linkage to the global optimal solution and compute the interval to the global optimum throughout the solution process.

A. Problem formulation

The equations used to represent the operation of a radial electrical distribution network [38]. The model is applied under the following assumptions: 1) the loads are modeled as constant active and reactive power. 2) In branch *i,j* the node *i* is closer to the substation node than node *j*. 3) The active and reactive power losses on branch *ij* are concentrated in origin node *i*. 4) The electrical distribution system is balanced and represented by a single-phase equivalent.

Objective function (10) maximizes SW which includes three terms. The first term represents the consumer benefit. The second term represents the cost of DR. Finally, the third term represents the generation cost for both active and reactive power of substation, WTs and PVs. In addition, QPF in the third term refers to the reactive power payment of WTs and PVs, which is nonlinear. Piecewise linearization approach is used to linearize the quadratic function in (10) [39].(see linearization section)

Maximize SW=

$$\left(\sum_{i=1}^{NB}\sum_{s=1}^{NS}\pi_s C_i^{l,P}P_{i,s}^{l}+\sum_{i=1}^{NB}\sum_{s=1}^{NS}\pi_s C_i^{l,Q}Q_{i,s}^{l}\right)-\left(\sum_{i=1}^{NB}\sum_{s=1}^{NS}C_i^{DR,P}P_{i,s}^{DR}+\sum_{i=1}^{NB}\sum_{s=1}^{NS}C_i^{DR,Q}Q_{i,s}^{DR}\right)-\left(\sum_{i=1}^{NB}\sum_{s=1}^{NS}C_i^{ss,P}P_{i,ss}^{ss}+\sum_{i=1}^{NB}\sum_{s=1}^{NS}C_i^{ss}Q_{i,s}^{ss}+\sum_{i=1}^{NB}\sum_{s=1}^{NS}\pi_s C_i^{w,P}P_{i,s}^{w}+\sum_{i=1}^{NB}\sum_{s=1}^{NS}\pi_s C_i^{pv,p}P_{i,s}^{pv}+\sum_{i=1}^{NB}QPF_i^{w,pv}\right) \quad (10)$$

B. Constraints

$$\sum_{i=1}^{NB}\sum_{s=1}^{NS}P_{i,s}^{ss}+\sum_{i=1}^{NB}\sum_{s=1}^{NS}P_{i,s}^{w}+\sum_{i=1}^{NB}\sum_{s=1}^{NS}P_{i,s}^{pv}+\sum_{i=1}^{NB}\sum_{s=1}^{NS}P_{i,s}^{DR}-\sum_{i=1}^{NB}\sum_{s=1}^{NS}P_{i,s}^{l}=\sum_{i=1}^{NB}\sum_{j=1}^{NB}\sum_{s=1}^{NS}(P_{i,j,s}+R_{i,j}I_{i,j,s}^{sq}) \quad (11)$$

$$\sum_{i=1}^{NB}\sum_{s=1}^{NS}Q_{i,s}^{ss}+\sum_{i=1}^{NB}\sum_{s=1}^{NS}Q_{i,s}^{w}+\sum_{i=1}^{NB}\sum_{s=1}^{NS}Q_{i,s}^{pv}+\sum_{i=1}^{NB}\sum_{s=1}^{NS}Q_{i,s}^{DR}-\sum_{i=1}^{NB}\sum_{s=1}^{NS}Q_{i,s}^{l}=\sum_{i=1}^{NB}\sum_{j=1}^{NB}\sum_{s=1}^{NS}(Q_{i,j,s}+X_{i,j}I_{i,j,s}^{sq}) \quad (12)$$

$$V_i^{sq}-V_j^{sq}-2\left[R_{i,j}(P_{i,j})+X_{i,j}\left(Q_{i,j}\right)\right]-Z_{i,j}^{2}I_{i,j}^{sq}=0 \quad (13)$$

$$T_{ss,i}V_{ss}^{sq}-V_j^{sq}-2\left[R_{i,j}\left(P_{j,i}\right)+X_{i,j}\left(Q_{j,i}\right)\right]-Z_{i,j}^{2}I_{i,j}^{sq}=0 \quad (14)$$

$$V_i^{sq}I_{i,j}^{sq}=P_{ij}^{2}+Q_{ij}^{2} \quad (15)$$

$$\left(V_i^{\min}\right)^2\le V_{i,s}^{sq}\le\left(V_i^{\max}\right)^2 \quad (16)$$

$$I_{i,j,s}^{sq}\le\left(I^{\max}\right)^2 y_{i,j,s} \quad (17)$$

$$P_i^{ss\,\min}\le P_{i,s}^{ss}\le P_i^{ss\,\max} \quad (18)$$

$$Q_i^{ss\,\min}\le Q_{i,s}^{ss}\le Q_i^{ss\,\max} \quad (19)$$

$$P_{i,s}^{w\,\min}\le P_{i,s}^{w}\le P_{i,s}^{w\max} \quad (20)$$

$$P_{i,s}^{PV\,\min}\le P_{i,s}^{PV}\le P_{i,s}^{PV\,\max} \quad (21)$$

$$Q_{i,s}^{w\,\min}\le Q_{i,s}^{w}\le Q_{i,s}^{w\max} \quad (22)$$

$$Q_{i,s}^{PV\,\min}\le Q_{i,s}^{PV}\le Q_{i,s}^{PV\,\max} \quad (23)$$

$$0\le P_{i,s}^{DR}\le P_{i,s}^{DR\max} \quad (24)$$

$$0\le Q_{i,s}^{DR}\le Q_{i,s}^{DR\max} \quad (25)$$

$$T_{i,j}^{\min}\le T_{i,j}\le T_{i,j}^{\max} \quad (26)$$

The above constraints can be categorized into two groups:

a) **Equality constraints**: Constraints (11)-(15) apply Kirchhoff's voltage law. Constraints (11)-(12) ensure the active and reactive power balances in system nodes. Eqs. (13)-(15) related to the active, reactive and apparent power flows and the current flow, where, V_i^{sq} is the square of voltage magnitude, $I_{i,j}^{sq}$ is the square of current magnitude. It is assumed that the lines with OLTC is modelled as series impedance R+jX with an ideal transformer with a variable turns ratio *T* as shown in Fig.4.

b) **Inequality constraints**: Constraint (16) determines the acceptable range of square voltage magnitude in nodes, while constraint (17) is the current flow limit in branch *i,j*. Constraints (18) and (19) set the upper bounds for active and reactive power

of substation. Constraints (20)-(23) limit the active and reactive power generations of WTs and PVs. Note that WTs and PVs generation depends on the solar irradiance and wind speed. DR constraints are introduced in Eqs.(24) and (25). Constraint (26) represents the limits of tap ratio in the OLTC.

C. The Structure of Reactive Power Offer

The reactive power capacity curve of PVs and WTs which is shown in Fig.3 (a) plays an important role to calculate its reactive power payment. In this figure, the framework of Q payment is classified into four operation regions as follows [17, 38][40];

Region 1(-Q_{mnd} to Q_{mnd}); if PVs and WTs operate in this area, it shall get only availability payment (mo) in pound per hour because it is operate according to the grid code requirement.

Region 2(Q^{min} to $-Q_{mnd}$), and Region 3 (Q_{mnd} to Q_{av}); if PVs and WTs operate in these areas, they expect to receive cost for losses (m_1) plus to the availability payment.

Region 4 (Q_{mnd} to Q^{max}); If PVs and WTs operate in this area, it must receive opportunity payments (m_2) besides the availability and losses payment because it miss the opportunity to sell active power. It is worth mentioning that the lost opportunity cost provided is a quadratic function.

Eqs. (27) and (28) explain the utmost obtainable reactive power generated by PVs and WTs and their capability curve respectively. Based on the framework payment of reactive power generation, Eq.29 introduce the payment function (QPF) of WTs and PVs reactive power. Notice that QPF formulation contains nonlinear part (see linearization section).

$$Q=\left\{\frac{\sqrt{(V_t+I_c)^2-(P^{w,pv})^2}}{\sqrt{\left(\frac{V_tV_c}{X_c}\right)^2-(P^{w,pv})^2}-\frac{V_t^2}{X_c}}\right\} \tag{27}$$

$$QPF=\begin{cases} m_0 & -Q_{mnd}\le Q_i^{2w,pv}\le Q_{mnd} \\ \frac{1}{2}m_1\left((Q_1)^2-(Q_{mnd})^2\right), & Q_1\le Q_i^{w,pv}\le -Q_{mnd} \\ \frac{1}{2}m_1\left((Q_2)^2-(Q_{mnd})^2\right), & Q_{mnd}\le Q^{w,pv}\le Q_2 \\ \left(\frac{1}{2}m_1\left((Q_{av})^2-(Q_{mnd})^2\right)+\right. & \\ \left.\frac{1}{2}m_2\left((Q_3)^2-(Q_{av})^2\right)\right., & Q_{mnd}\le Q^{w,pv}\le Q_{av}, Q_{av}\le Q^{w,pv}\le Q_3 \end{cases} \tag{28}$$

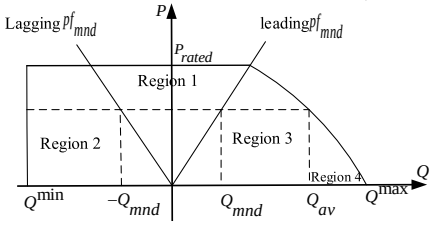

(a)

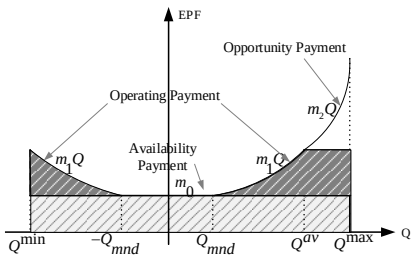

(b)

Fig.3. (a) Capability curve, (b) The offer structure of reactive power

$$QPF = Z_0m_0 + Z_1\frac{1}{2}m_1\left((Q_1)^2-(Q_{mnd})^2\right) + Z_2\frac{1}{2}m_1\left((Q_2)^2-(Q_{mnd})^2\right) + Z_3\left[\frac{1}{2}m_1\left((Q_{av})^2-(Q_{mnd})^2\right)+\frac{1}{2}m_2\left((Q_3)^2-(Q_{av})^2\right)\right] \tag{29}$$

The binary variables (Z_0, Z_1, Z_2, and Z_3) are regulating the PVs and WTs region in order to compensate it. If accepted unit participates in any of the following areas then the binary variables values will be as follows

.

region 1,	$Z_0=1$,	$Z_1=Z_2=Z_3=0$;
region 2,	$Z_0=Z_1=1$,	$Z_2=Z_3=0$;
region 3,	$Z_0=Z_2=1$,	$Z_1=Z_3=0$;
region 4,	$Z_0=Z_2=Z_3=1$,	$Z_1=0$;

The PVs and WTs equality and inequality constraints are presented as below.

$$Z_0, Z_1, Z_2, Z_3 \in \{0,1\} \tag{30}$$

$$-Z_0Q_{mnd}^{w,pv} \le Q_0^{w,pv} \le Z_0Q_{mnd}^{w,pv} \tag{31}$$

$$Z_1Q_{\min}^{w,pv} \le Q_1^{w} \le -Z_1Q_{mnd}^{w,pv} \tag{32}$$

$$Z_2Q_{mnd}^{w,pv} \le Q_2^{w,pv} \le Z_2Q_{av}^{w,pv} \tag{33}$$

$$Z_3Q_{av}^{w,pv} \le Q_3^{w,pv} \le Z_3Q_{\max}^{w,pv} \tag{34}$$

$$Q_{mnd}^{w,pv} = P^{W,PV}\tan\left(\cos^{-1}\left(pf_{mnd}\right)\right) \tag{35}$$

$$Q^{w,pv} = Q_0^{w,pv} + Q_1^{w,pv} + Q_2^{w,pv} + Q_3^{w,pv} \tag{36}$$

$$Z_1 + Z_2 + Z_3, \le Z_0 \tag{37}$$

A cap on the reduction in the active power is imposed in order to minimize the impact of reactive power dispatch on the initial active WTs and PVs dispatch power $P_i^{w,pv,ini}$.

$$\Delta P_i^{w,pv} \le x_i^{w,pv}P_i^{w,pv,ini} \tag{38}$$

where $x_i^{w,pv}$ is the considered cap on reduction in active power of WTs and PVs.

D. Linearization

To avoid nonlinearity, the linearization process described in [39, 41] is used.

1) The component QPF in Eq.10 contains nonlinear part, in order to linearize it, first order approximation is used [39]. Equations (39)-(43) describe the linearization process as follows:

$$Q^2 = \sum_{l=1}^{L}(2l-1)\frac{Q^{\max}}{L}\Delta Q_l \tag{39}$$

$$Q^+ - Q^- = Q \tag{40}$$

$$Q^+ + Q^- = \sum \Delta Q_l \tag{41}$$

$$Q^+ \ge 0;\ Q^- \ge 0 \tag{42}$$

$$\Delta Q_l \ge \Delta Q_{l+1} \tag{43}$$

In Eq. 39, piecewise linear approximation is used to linearize the quadratic variable by considering L segments. The flow

variable is divided into two parts, positive (forward) variables and negative (reverse) auxiliary flow variables. This is to enable only the use of the first quadrant in the quadratic curve as explained in Eq.40. Eq.41 guarantees that the step flow variables ΔQ_l and the flow are equal. It is worthy to note that these variables are impossible to be non-negative and nonzero simultaneously as enforced by (42). Eq. 43 ensures the successive filling of the partitions.

2) $T_{ss,i}V_{ss}^{sq}$ is nonlinear in eq (14). The same above linearization method is provided as follows:

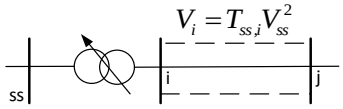

Fig.4. Line model

$$\kappa_{ss,i} = \frac{T_{ss,i} - u_{ss,i}}{2} \quad (44)$$

$$\omega_{ss,i} = \frac{T_{ss,i} - u_{ss,i}}{2} \quad (45)$$

where $\omega_{ss,i} - \kappa_{ss,i} = T_{ss,i}u_{ss}$ (46)

$$\kappa_{ss,i} = \kappa_{ss,i}^{+} - \kappa_{ss,i}^{-} \quad (47)$$

$$\kappa_{ss,i}^{+} - \kappa_{ss,i}^{-} = \sum_f \Delta\kappa_{ss,i,f} \quad (48)$$

$$\kappa_{ss,i,f}^2 = \sum_f (2f-1)\Delta\kappa_{ss,i}^{\max}\Delta\kappa_{ss,i,f} \quad (49)$$

$$0 \le \kappa_{ss,i,f} \le \Delta\kappa_{ss,i}^{\max} \quad (50)$$

where $\Delta\kappa_{ss,i}^{\max} = \frac{\kappa_{ss,i}^{\max}}{F}$ (51)

$$\omega_{ss,i} = \omega_{ss,i}^{+} - \omega_{ss,i}^{-} \quad (52)$$

$$\omega_{ss,i}^{+} - \omega_{ss,i}^{-} = \sum_f \Delta\omega_{ss,i,f} \quad (53)$$

$$\omega_{ss,i,f}^2 = \sum_f (2f-1)\Delta\omega_{ss,i}^{\max}\Delta\omega_{ss,i,f} \quad (54)$$

$$0 \le \omega_{ss,i,f} \le \Delta\omega_{ss,i}^{\max} \quad (55)$$

where $\Delta\omega_{ss,i}^{\max} = \frac{\omega_{ss,i}^{\max}}{F}$ (56)

3) $V_i^{sq}I_{i,j}^{sq} = P_{ij}^2 + Q_{ij}^2$: both the left and right sides are nonlinear and both should be linearized separately [42]. Note that V_i^{sq} and $I_{i,j}^{sq}$ are variables that represent the square magnitude values of voltages and currents, respectively.

- $V_j^{sq}I_{i,j}^{sq}$: The product of two variables is linearized by discretizing V_i^{sq} in small intervals. However, this leads to an increase in the number of binary variables and computation time. Since the voltage magnitude is within small range in electrical distribution systems, a constant value V_{nom}^{sqr} is selected and substituted for V_j^{sq} in equation 15 for the first iteration. Then, the model is run again and V_j^{sq} takes the value resulting from the first iteration. Note that V_j^{sq} hardly changes after the second iteration.
- $P_{ij}^2 + Q_{ij}^2$: the linearization of both terms on the right side of (15) is carried out by a piecewise linear approximation, as follows:

$$P_{ij}^2 + Q_{ij}^2 = \sum(m_{i,j}\Delta P_{i,j}) + \sum(m_{i,j}\Delta Q_{i,j}) \quad (57)$$

$$P_{i,j}^{+} - P_{i,j}^{-} = P_{i,j} \quad (58)$$

$$Q_{i,j}^{+} - Q_{i,j}^{-} = Q_{i,j} \quad (59)$$

$$P_{i,j}^{+} + P_{i,j}^{-} = \sum \Delta P_{i,j} \quad (60)$$

$$Q_{i,j}^{+} + Q_{i,j}^{-} = \sum \Delta Q_{i,j} \quad (61)$$

$$0 \le \Delta P_{i,j} \le \Delta S_{i,j} \quad (62)$$

$$0 \le \Delta Q_{i,j} \le \Delta S_{i,j} \quad (63)$$

$$P_{i,j}^{+} \le V_{nom}I_{i,j}^{\max}o_{i,j}^{P+} \quad (64)$$

$$P_{i,j}^{-} \le V_{nom}I_{i,j}^{\max}o_{i,j}^{P-} \quad (65)$$

$$Q_{i,j}^{+} \le V_{nom}I_{i,j}^{\max}o_{i,j}^{Q+} \quad (66)$$

$$Q_{i,j}^{-} \le V_{nom}I_{i,j}^{\max}o_{i,j}^{Q-} \quad (67)$$

Eq. 57 is a linear approximation of $P_{ij}^2 + Q_{ij}^2$ .To ensure that $P_{i,j}^{+} + P_{i,j}^{-}$ and $Q_{i,j}^{+} + Q_{i,j}^{-}$ are equal to the sum of all values in separated blocks, Eqs. (58) and (61) are represented. Both upper and lower bounds of the variable are represented Eqs. (62) and (63). Constraints (64)-(67) are introduced for active and reactive power constraints. Parameters $I_{i,j}^{\max}$ and V_{nom} are Maximum current flow in branches *i* and *j* and nominal voltage of the distribution network. In addition, $o_{i,j}^{P+}$, $o_{i,j}^{P+}$, $o_{i,j}^{P-}$, $o_{i,j}^{Q+}$ $o_{i,j}^{Q-}$ are binary variables to avoid considering forward and backward power flow simultaneously. Note that the slope $m_{i,j}$ and the variation $\Delta S_{i,j}$ are constant parameters which are defined as follow

$$m_{i,j} = (2r-1)\Delta S_{i,j} \quad (68)$$

$$\Delta S_{i,j} = (V_{nom}I_{i,j}^{\max})/R^{tot} \quad (69)$$

As shown in (57)–(61), the right side of (15) can be replaced with the right side of (57) to form a linear equation. The linear form of (15) is shown as follow which V_i^{sq} is constant and $\sum(m_{i,j}\Delta P_{i,j})$ and $\sum(m_{i,j}\Delta Q_{i,j})$ are linear approximation of P_{ij}^2 and Q_{ij}^2 ;

$$V_i^{sq}I_{i,j}^{sq} = \sum(m_{i,j}\Delta P_{i,j}) + \sum(m_{i,j}\Delta Q_{i,j}) \quad (70)$$

The linearization processes performed in the proposed method is illustrated in Fig.5.

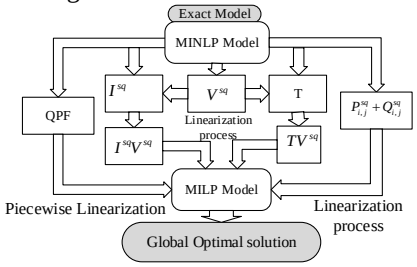

Fig.5. Illustration of the linearization processes performed in the proposed method

Linear model is used as a benchmark against which the approximate nonlinear model can be compared. In this regard, first the linear model is solved and the global optimal solution of the problem is found. This solution is then used as a benchmark for assessing the solution accuracy of the nonlinear model. Note that, the accuracy evaluation of the MILP model was conducted based on the error in the SW. In addition, the error computation time is used, as shown in Eq. 71, as an index for evaluation of the performance of the proposed model. Note that the error indicates the deviation of the nonlinear model from the global solution which is found by linear model, it is noted that the error is 0.23% in the SW. In addition, The computational time required for solving the nonlinear and linear models are respectively 1.484 and 0.938 min.

$$Error = \frac{t^{nonlinear} - t^{linear}}{t^{linear}} \times 100\% \quad (71)$$

where $t^{nonlinear}$ and t^{linear} denote the time associated with the nonlinear and linear models, respectively.

IV. Case Study

A 16-bus 33-kV UK generic distribution system (UKGDS) is used for numerical analysis [43], as illustrated in Fig.6.

In order to assess the impact of wind and solar power penetration on active and reactive D-LMPs with ANM schemes and DR, three WTs and two PVs units are installed in the distribution network. The candidate buses for WTs are buses 5, 10, and 13 with the nominal capacity of 660,440 and 880 kW, respectively and PVs are 2 and 11 with the nominal capacity of 660 and 440 kW, respectively. The upper and lower limit of voltage at each is assumed to be 1.06 and 0.94 p.u. The total active and reactive peak demand are 38.2MW and 7.7 MVAr. Table 2 presents active and reactive load demands bid prices and it is assumed that there are three blocks for each load at maximum demand [44, 45] . The offer prices for active and reactive power supplied by the substation are 150 £/MWh and 70 £/MVArh, respectively. The proposed method has been solved as mixed-integer linear programming (MILP) problem on a PC with Core i7 CPU and 16 GB of RAM using CPLEX under GAMS software [46]. The stopping criterion for the branch and-cut algorithm of CPLEX used in the proposed model is based on an optimality gap equal to 0.5%.

TABLE 2
ACTIVE AND REACTIVE POWER BID PRICES FOR THE LOADS

Bus No.	Active power bid price list			Reactive power bid price list		
	Blocks (MW@£/MWh)			Blocks MVAr@£/MVArh		
	b_1	b_2	b_3	b1	b2	b3
2	2.51@280	1.90@260	1.01@250	0.600@200	0.300@230	0.190@200
3	1.10@260	0.70@250	0.13@230	0.210@180	0.120@205	0.060@195
4	0.02@260	0.03@250	0.01@240	0.004@180	0.0035@210	0.0025@20
5	9.18@250	6.12@240	3.10@230	2.110@170	1.200@120	0.430@180
6	1.9@240	0.61@230	0.26@230	0.210@160	0.140@195	0.050@185
7	0.91@250	0.59@220	0.40@220	0.200@170	0.110@185	0.080@175
9	0.21@220	0.2@220	0.15@220	0.060@140	0.030@180	0.020@180
10	1.41@220	0.89@210	0.40@200	0.225@140	0.185@175	0.150@155
11	1.50@210	0.90@200	0.45@200	0.300@135	0.200@155	0.080@160
12	0.45@220	0.21@200	0.15@190	0.080@140	0.070@165	0.030@145
13	0.69@200	0.21@190	0.11@170	0.100@120	0.070@145	0.030@135
14	0.35@190	0.15@180	0.08@170	0.060@115	0.040@153	0.020@130

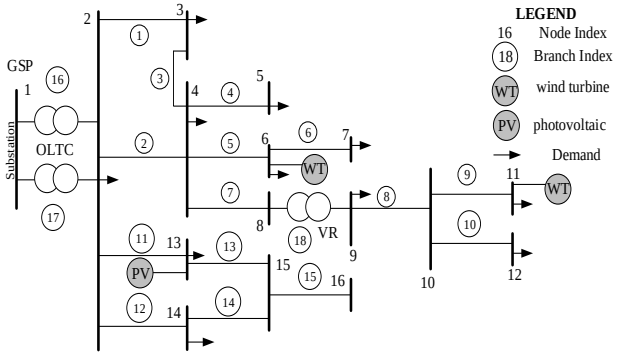

Fig.6. 16-bus 33-kV UKGDS

TABLE 3
FINANCIAL DATA FOR APPROXIMATING OFFER PRICE OF ACTIVE POWER GENERATED BY PVs AND WTs

Size	WTs	PVs
Installation cost (£/kW)	1200	1400
Number of equivalent hours (h)	4000	4000
Interest rate (%)	3	3
Depreciation time (years)	3	3
Capacity factor (%)	46	46
Annual cost (£/kW-year)	168.81	229.77
Active Offer Price (£/MWh)	**35.16**	**41.03**

A. Calculation the active power quantity and the offer prices of PVs and WTs

According to financial data provides in Table 3, WTs' and PVs' active power prices are calculated [44, 47]. Eq.72 introduces the annual cost formula to calculate PVs and WTs offer prices as follows:

$$Ann\_Cost = \frac{r(1+r)^n}{(1+r)^n - 1} \times Inst\_Cost \quad (72)$$

where *Ann_Cost* is the annual cost of depreciation, *n* and *r* are the depreciation period in the year and the interest rate in (%) respectively, *Inst_Cost* is the installation cost. According to the capability curve of PVs and WTs and their data, the capacity factor is assessed. The offer price of active power generated by PVs and WTs is calculated by dividing *Ann_Cost* by total number of hours.

B. Calculation of the reactive power and energy adjustment offer prices of PVs and WTs

According to the QPF of PVs and WTs, Table 4 lists the reactive offer prices.

TABLE 4
OFFER PRICES OF REACTIVE POWER GENERATED BY PVs AND WTs

	Q_{max} kVAr	Q_{min} KVAr	m_0 (£)	m_1 (£/MVar)	m_2 (£/MVar h)^2	m_{adj} £/MVar	X %
WTs	630	-220	0.082	0.015	0.35×10^{-3}	0.068	30
PVs	270	-60	0.068	0.013	0.42×10^{-3}	0.072	30

V. Simulation Results

It is worth mentioning that the correlation between uncertainties characterizing associated with load demand, wind speed, and solar irradiation has been considered by using Scenario-Tree approach. For the present paper, jointly

considering four-time blocks, three load demand levels, three wind speed levels, three solar irradiation levels, which are leading to 108 different scenarios. The same correlation among load demand and wind and PV power production is considered in all the locations of the system. Table 5 provides the characteristics of load demand, wind speed and solar irradiance scenarios.

TABLE 5
LOAD DEMAND, WT AND PV SCENARIOS

Scenarios	Demand block	Number of Hours	Demand level	Wind	Solar
1	1	1200	0.967	0.436	0.336
2			0.967	0.436	0.167
3			0.967	0.436	0.102
4			0.967	0.267	0.336
5			0.967	0.267	0.167
6			0.967	0.267	0.102
7			0.967	0.122	0.336
8			0.967	0.122	0.167
9			0.967	0.122	0.102
10			0.921	0.436	0.336
11			0.921	0.436	0.167
12			0.921	0.436	0.102
13			0.921	0.267	0.336
14			0.921	0.267	0.167
15			0.921	0.267	0.102
16			0.921	0.122	0.336
17			0.921	0.122	0.167
18			0.921	0.122	0.102
19			0.875	0.436	0.336
20			0.875	0.436	0.167
21			0.875	0.436	0.102
22			0.875	0.267	0.336
23			0.875	0.267	0.167
24			0.875	0.267	0.102
25			0.875	0.122	0.336
26			0.875	0.122	0.167
27			0.875	0.122	0.102
28	2	3600	0.873	0.401	0.301
29			0.873	0.401	0.223
30			0.873	0.401	0.102
31			0.873	0.223	0.301
32			0.873	0.223	0.223
33			0.873	0.223	0.102
34			0.873	0.122	0.301
35			0.873	0.122	0.223
36			0.873	0.122	0.102
37			0.831	0.401	0.301
38			0.831	0.401	0.223
39			0.831	0.401	0.102
40			0.831	0.223	0.301
41			0.831	0.223	0.223
42			0.831	0.223	0.102
43			0.831	0.122	0.301
44			0.831	0.122	0.223
45			0.831	0.122	0.102
46			0.789	0.401	0.301
47			0.789	0.401	0.223
48			0.789	0.401	0.102
49			0.789	0.223	0.301
50			0.789	0.223	0.223
51			0.789	0.223	0.102
52			0.789	0.122	0.301
53			0.789	0.122	0.223
54			0.789	0.122	0.102
55	3	2400	0.793	0.365	0.265
56			0.793	0.365	0.223
57			0.793	0.365	0.092
58			0.793	0.223	0.265
59			0.793	0.223	0.223
60			0.793	0.223	0.092
61			0.793	0.112	0.265
62			0.793	0.112	0.223
63			0.793	0.112	0.092
64			0.755	0.365	0.265
65			0.755	0.365	0.223
66			0.755	0.365	0.092
67			0.755	0.223	0.265
68			0.755	0.223	0.223
69			0.755	0.223	0.092
70			0.755	0.112	0.265
71			0.755	0.112	0.223
72			0.755	0.112	0.092
73			0.717	0.365	0.265
74			0.717	0.365	0.223
75			0.717	0.365	0.092
76			0.717	0.223	0.265
77			0.717	0.223	0.223
78			0.717	0.223	0.092
79			0.717	0.112	0.265
80			0.717	0.112	0.223
81			0.717	0.112	0.092
82	4	1560	0.682	0.351	0.251
83			0.682	0.351	0.174
84			0.682	0.351	0.085
85			0.682	0.194	0.251
86			0.682	0.194	0.174
87			0.682	0.194	0.085
88			0.682	0.095	0.251
89			0.682	0.095	0.174
90			0.682	0.095	0.085
91			0.649	0.351	0.251
92			0.649	0.351	0.174
93			0.649	0.351	0.085
94			0.649	0.194	0.251
95			0.649	0.194	0.174
96			0.649	0.194	0.085
97			0.649	0.095	0.251
98			0.649	0.095	0.174
99			0.649	0.095	0.085
100			0.617	0.351	0.251
101			0.617	0.351	0.174
102			0.617	0.351	0.085
103			0.617	0.194	0.251
104			0.617	0.194	0.174
105			0.617	0.194	0.085
106			0.617	0.095	0.251
107			0.617	0.095	0.174
108			0.617	0.095	0.085

This section discusses the results from three case studies shown in Table 6, which will facilitate to study the impact of ANM schemes and DR on SW, dispatched active and reactive power, and active and reactive D-LMPs. For each case, the SW, the total dispatched active and reactive power for WTs and PVs, and the total active and reactive D-LMPs at candidate buses are examined.

Figs. 7 and 8 show the total dispatched active and reactive power supplied by WTs and PVs for each cases at candidate buses. It is evident that buses 11 and 13 have the lowest and highest dispatched active and reactive power respectively supplied by WTs and PVs. This is due to active and reactive bid prices and voltage thermal limits at each bus. At the same time, it can be observed in these figures that in case C (with ANM schemes and DR), the total dispatched active and reactive power of WTs and PV is higher compared with those in case A and B by up to 20% for active power and up to 13% for reactive power. Fig. 9 shows the SW for three cases. It is seen that case C has the highest SW compared with those in case A and case B. This is mainly due to the higher dispatched active and reactive power in case C with integration of ANM schemes and DR, which allows increasing the SW.

TABLE 6. CASES

Case	ANM	DR
A	×	×
B	✓	×
C	✓	✓

Table 7 and Fig. 10 show the total active and reactive D-LMPs at candidate buses in all cases. It indicates that a highest active D-LMPs is related to bus 11 and lowest active D-LMP is related to bus 13; this is due to the highest and lowest dispatched active and reactive power of WTs and PVs at these buses. It should be noted that the active and reactive D-LMPs in case C is decreased if compared with those in case A and B by up to 1.5% and 6%, respectively. This mainly due to ANM schemes and DR program. To further clarify the impact of ANM schemes and DR on the system voltages and current, Figs. 11 and 12 are presented. It is evident from Fig.11 that bus 13 has the highest voltage this which is related to the highest reactive power at bus 13.

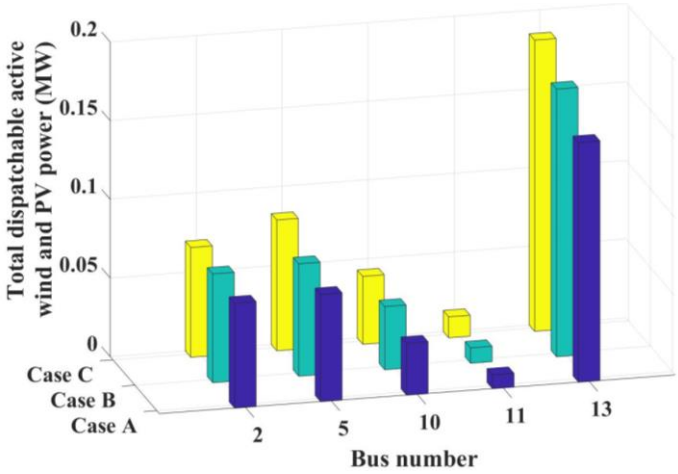

Fig.7. Total dispatched active wind and solar power at candidate buses in all cases.

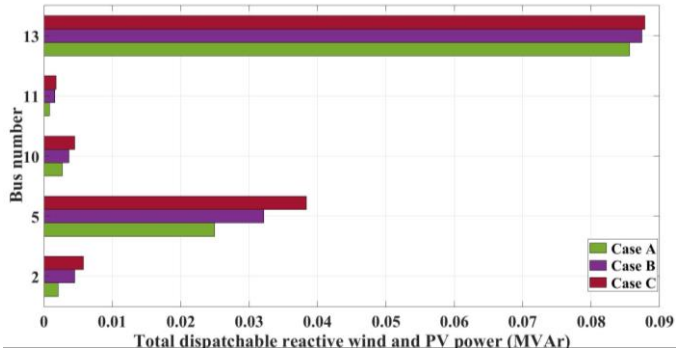

Fig.8. Total dispatched reactive wind and PV power at candidate buses in all cases

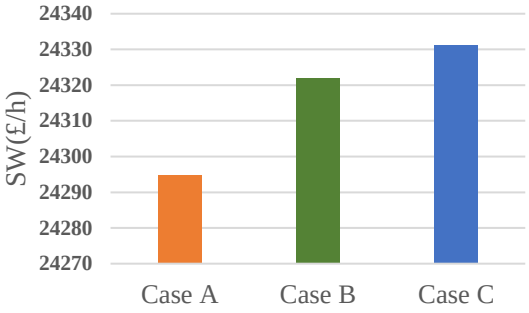

Fig.9. Social welfare for each case

TABLE 7
TOTAL ACTIVE D-LMP AT CANDIDATE BUSES FOR ALL CASES

	Bus No.	Total active D-LMP((£/MWh)
Case A	2	8850.143
	5	9252.783
	10	9499.11
	11	9892.786
	13	8206.665
Case B	2	8752.238
	5	9201.512
	10	9370.11
	11	9820.03
	13	8103.081
Case C	2	8711.999
	5	9116.291
	10	9330.038
	11	9649.589
	13	8003.495

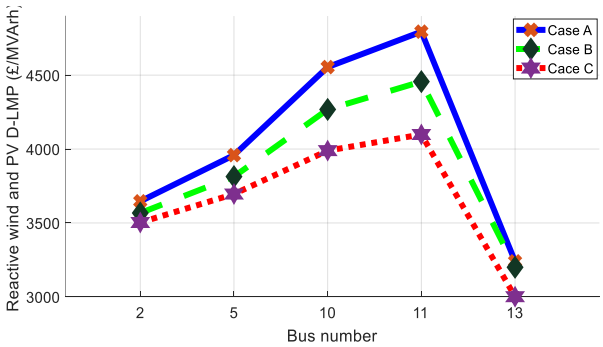

Fig.10. Total reactive D-LMP at candidate buses for all cases

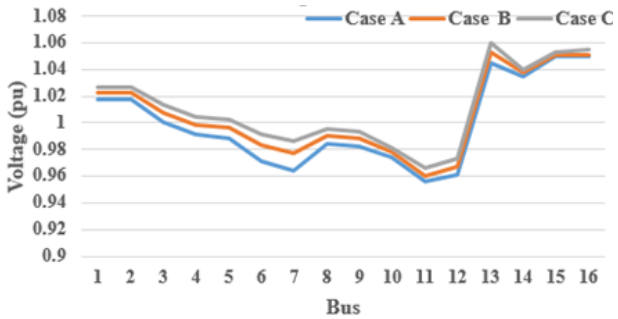

Fig. 11. Voltage profile at all buses

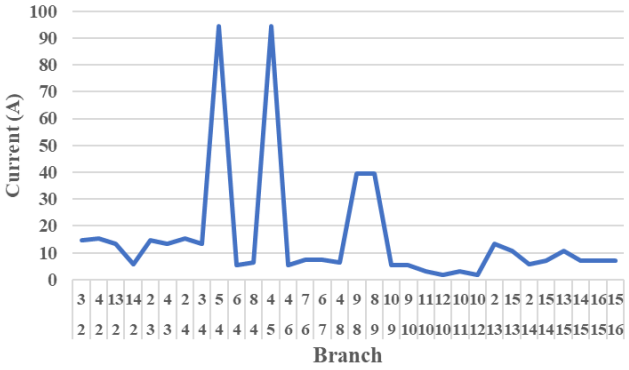

Fig. 12 Current profile of the system

VI. CONCLUSION

In this paper, a novel approach is proposed for optimal operation of distribution network within a joint active and reactive electricity market incorporating active network management schemes and demand response. Market-based active and reactive optimal power flow is utilized to maximize the social welfare. To assess the WTs and PVs power penetration and their effects on social welfare as well as on active and reactive D-LMP prices. A stochastic approach is employed taking into account the uncertainties associated with wind speed, photovoltaics irradiance and load demand. Scenario-tree method is used to model the abovementioned uncertainties.

The proposed method can assist DNOs to evaluate the influence of wind and solar power generation on a network, specifically, technical and economic impacts. This technique will also assist DNOs to install WTs and PVs at more suitable locations in terms of cost minimization and benefiting consumers. It is capable to provide precise and real-time pricing which clears the way to manage the suggested market more, effectively which leads to total cost reduction. This shows the engagement of DNOs and consumers in the distribution market, and utilizing the active and reactive D-LMPs.

AKNOWLEDGMENTS

The authors wish to greatly thanks the finincial support from the Ministry of Higher Education Scientific Research in Iraq.

AUTHORS AFFILIATION

(Corresponding author: Rana H.A. Zubo).
Rana H.A. Zubo, Geev Mokryani, are with the School of Electrical Engineering and Computer Science, University of Bradford, Bradford BD7 1DP, U.K. In addition Rana is also with Kirkuk Technical College, Kirkuk, Iraq.
(e-mail: r.h.a.zubo@bradford.ac.uk; g.mokryani@bradford.ac.uk;

REFERENCES

[1] S. Xie *et al.*, "Multi-objective active distribution networks expansion planning by scenario-based stochastic programming considering uncertain and random weight of network," *Applied Energy*, vol. 219, pp. 207-225, 2018.
[2] R. Palma-Behnke, L. S. Vargas, and A. Jofré, "A distribution company energy acquisition market model with integration of distributed generation and load curtailment options," *IEEE Transactions on Power Systems*, vol. 20, no. 4, pp. 1718-1727, 2005.
[3] T. Soares, R. J. Bessa, P. Pinson, and H. Morais, "Active distribution grid management based on robust AC optimal power flow," *IEEE Transactions on Smart Grid*, 2017.
[4] R. H. Zubo, G. Mokryani, H.-S. Rajamani, J. Aghaei, T. Niknam, and P. Pillai, "Operation and planning of distribution networks with integration of renewable distributed generators considering uncertainties: A review," *Renewable and Sustainable Energy Reviews*, vol. 72, pp. 1177-1198, 2017.
[5] A. Saint-Pierre and P. Mancarella, "Active distribution system management: a dual-horizon scheduling framework for DSO/TSO interface under uncertainty," *IEEE Transactions on Smart Grid*, vol. 8, no. 5, pp. 2186-2197, 2017.
[6] G. Mokryani, Y. F. Hu, P. Papadopoulos, T. Niknam, and J. Aghaei, "Deterministic approach for active distribution networks planning with high penetration of wind and solar power," *Renewable Energy*, vol. 113, pp. 942-951, 2017.
[7] H. Gao, J. Liu, and L. Wang, "Robust coordinated optimization of active and reactive power in active distribution systems," *IEEE Transactions on Smart Grid*, 2017.
[8] S. S. AlKaabi, V. Khadkikar, and H. Zeineldin, "Incorporating PV inverter control schemes for planning active distribution networks," *IEEE Transactions on Sustainable Energy*, vol. 6, no. 4, pp. 1224-1233, 2015.
[9] M. H. Albadi and E. F. El-Saadany, "A summary of demand response in electricity markets," *Electric power systems research*, vol. 78, no. 11, pp. 1989-1996, 2008.
[10] Y. Rebours, D. Kirschen, and M. Trotignon, "Fundamental design issues in markets for ancillary services," *The Electricity Journal*, vol. 20, no. 6, pp. 26-34, 2007.
[11] J. P. Roselyn, D. Devaraj, and S. S. Dash, "Voltage-based reactive power pricing in deregulated environment using hybrid multi-objective particle swarm optimisation," *International Journal of Ambient Energy*, vol. 39, no. 3, pp. 285-296, 2018.
[12] E. L. Miguélez, I. E. Cortés, L. R. Rodríguez, and G. L. Camino, "An overview of ancillary services in Spain," *Electric Power Systems Research*, vol. 78, no. 3, pp. 515-523, 2008.
[13] F. Echavarren, E. Lobato, and L. Rouco, "Steady-state analysis of the effect of reactive generation limits in voltage stability," *Electric Power Systems Research*, vol. 79, no. 9, pp. 1292-1299, 2009.
[14] R. Doherty, G. Lalor, and M. O'Malley, "Frequency control in competitive electricity market dispatch," *IEEE Transactions on Power Systems*, vol. 20, no. 3, pp. 1588-1596, 2005.
[15] E. Ela, V. Gevorgian, A. Tuohy, B. Kirby, M. Milligan, and M. O'Malley, "Market designs for the primary frequency response ancillary service—Part II: Case studies," *IEEE Transactions on Power Systems*, vol. 29, no. 1, pp. 432-440, 2014.
[16] C. Liu and P. Du, "Participation of Load Resources in Day-ahead Market to Provide Primary-Frequency Response Reserve," *IEEE Transactions on Power Systems*, 2018.
[17] N. Amjady, A. Rabiee, and H. Shayanfar, "Pay-as-bid based reactive power market," *Energy Conversion and Management*, vol. 51, no. 2, pp. 376-381, 2010.
[18] A. Rabiee, H. Shayanfar, and N. Amjady, "Multiobjective clearing of reactive power market in deregulated power systems," *Applied energy*, vol. 86, no. 9, pp. 1555-1564, 2009.
[19] S. S. Reddy, A. Abhyankar, and P. Bijwe, "Reactive power price clearing using multi-objective optimization," *Energy*, vol. 36, no. 5, pp. 3579-3589, 2011.
[20] A. Samimi and A. Kazemi, "Scenario-based stochastic programming for Volt/Var control in distribution systems with renewable energy sources," *IETE Technical Review*, vol. 33, no. 6, pp. 638-650, 2016.
[21] C. Cecati, C. Citro, and P. Siano, "Combined operations of renewable energy systems and responsive demand in a smart grid," *IEEE Transactions on Sustainable Energy*, vol. 2, no. 4, pp. 468-476, 2011.
[22] A. C. Rueda-Medina and A. Padilha-Feltrin, "Distributed generators as providers of reactive power support—A market approach," *IEEE Transactions on Power Systems*, vol. 28, no. 1, pp. 490-502, 2013.
[23] L. Bai, J. Wang, C. Wang, C. Chen, and F. F. Li, "Distribution Locational Marginal Pricing (DLMP) for Congestion Management and Voltage Support," *IEEE Transactions on Power Systems*, 2017.
[24] A. P. C. de Mello, L. L. Pfitscher, and D. P. Bernardon, "Coordinated Volt/VAr control for real-time operation of smart distribution grids," *Electric Power Systems Research*, vol. 151, pp. 233-242, 2017.
[25] S. Ikeda and H. Ohmori, "Evaluation for Maximum Hosting Capacity of Distributed Generation considering Active Network Management," *International Journal of Electrical and Electronic Engineering and Telecommunications*, vol. 7, no. 3, pp. 96-102, 2018.
[26] Y. He and M. Petit, "Demand response scheduling to support distribution networks operation using rolling multi-period optimization," *Journal of Process Control*, 2018.
[27] C. De Jonghe, B. F. Hobbs, and R. Belmans, "Optimal generation mix with short-term demand response and wind penetration," *IEEE Transactions on Power Systems*, vol. 27, no. 2, pp. 830-839, 2012.
[28] M. J. Ghadi, S. Ghavidel, A. Rajabi, A. Azizivahed, L. Li, and J. Zhang, "A review on economic and technical operation of active distribution systems," *Renewable and Sustainable Energy Reviews*, vol. 104, pp. 38-53, 2019.

[29] L. F. Ochoa, C. J. Dent, and G. P. Harrison, "Distribution network capacity assessment: Variable DG and active networks," *IEEE Transactions on Power Systems*, vol. 25, no. 1, pp. 87-95, 2010.
[30] S. S. Reddy, A. Abhyankar, and P. Bijwe, "Market clearing for a wind-thermal power system incorporating wind generation and load forecast uncertainties," in *Power and Energy Society General Meeting, 2012 IEEE*, 2012, pp. 1-8: IEEE.
[31] Y. M. Atwa and E. F. El-Saadany, "Probabilistic approach for optimal allocation of wind-based distributed generation in distribution systems," *IET Renewable Power Generation*, vol. 5, no. 1, pp. 79-88, 2011.
[32] S. S. Reddy, B. Panigrahi, R. Kundu, R. Mukherjee, and S. Debchoudhury, "Energy and spinning reserve scheduling for a wind-thermal power system using CMA-ES with mean learning technique," *International Journal of Electrical Power & Energy Systems*, vol. 53, pp. 113-122, 2013.
[33] S. S. Reddy and J. A. Momoh, "Realistic and transparent optimum scheduling strategy for hybrid power system," *IEEE Transactions on Smart Grid*, vol. 6, no. 6, pp. 3114-3125, 2015.
[34] H. Falaghi, M. Ramezani, C. Singh, and M.-R. Haghifam, "Probabilistic assessment of TTC in power systems including wind power generation," *IEEE Systems Journal*, vol. 6, no. 1, pp. 181-190, 2012.
[35] S. Montoya-Bueno, J. Muñoz-Hernández, and J. Contreras, "Uncertainty management of renewable distributed generation," *Journal of Cleaner Production*, vol. 138, pp. 103-118, 2016.
[36] S. S. Reddy, P. Bijwe, and A. R. Abhyankar, "Joint energy and spinning reserve market clearing incorporating wind power and load forecast uncertainties," *IEEE Systems Journal*, vol. 9, no. 1, pp. 152-164, 2015.
[37] S. S. Reddy, P. Bijwe, and A. R. Abhyankar, "Optimal posturing in day-ahead market clearing for uncertainties considering anticipated real-time adjustment costs," *IEEE Systems Journal*, vol. 9, no. 1, pp. 177-190, 2015.
[38] J. F. Franco, M. J. Rider, and R. Romero, "A mixed-integer quadratically-constrained programming model for the distribution system expansion planning," *International Journal of Electrical Power & Energy Systems*, vol. 62, pp. 265-272, 2014.
[39] S. F. Santos *et al.*, "Impacts of operational variability and uncertainty on distributed generation investment planning: A comprehensive sensitivity analysis," *IEEE Transactions on Sustainable Energy*, vol. 8, no. 2, pp. 855-869, 2017.
[40] S. Pirouzi, J. Aghaei, M. A. Latify, G. R. Yousefi, and G. Mokryani, "A robust optimization approach for active and reactive power management in smart distribution networks using electric vehicles," *IEEE Systems Journal*, vol. 12, no. 3, pp. 2699-2710, 2017.
[41] J. F. Franco, M. J. Rider, M. Lavorato, and R. Romero, "A mixed-integer LP model for the optimal allocation of voltage regulators and capacitors in radial distribution systems," *International Journal of Electrical Power & Energy Systems*, vol. 48, pp. 123-130, 2013.
[42] P. M. de Quevedo, J. Contreras, M. J. Rider, and J. Allahdadian, "Contingency assessment and network reconfiguration in distribution grids including wind power and energy storage," *IEEE Transactions on Sustainable Energy*, vol. 6, no. 4, pp. 1524-1533, 2015.
[43] "Distibuted Generation and Sustainable Electrical Energy Center,United Kingdom Generic Distribution System (UK GDS). [Online]." *Available* <*http://www.sedg.ac.uk/*>.
[44] A. G. Tsikalakis and N. D. Hatziargyriou, "Centralized control for optimizing microgrids operation," in *Power and Energy Society General Meeting, 2011 IEEE*, 2011, pp. 1-8: IEEE.
[45] R. H. Zubo, G. Mokryani, and R. Abd-Alhameed, "Optimal operation of distribution networks with high penetration of wind and solar power within a joint active and reactive distribution market environment," *Applied energy*, vol. 220, pp. 713-722, 2018.
[46] A. Brooke, D. Kendrick, A. Meeraus, R. Raman, and U. America, "The general algebraic modeling system," *GAMS Development Corporation*, vol. 1050, 1998.
[47] P. Siano and G. Mokryani, "Evaluating the benefits of optimal allocation of wind turbines for distribution network operators," *IEEE Systems Journal*, vol. 9, no. 2, pp. 629-638, 2013.

Rana Zubo (M'01) was born in Iraq and she received the B.Sc and the M.Sc degrees in Electrical Engineering from The University of Technology, Baghdad, Iraq in 1998 and 2006, respectively. She has worked in Kirkuk Technical College, Iraq as a Lecturer from 1999 to 2015 and then she received a scholarship from the Iraqi government to continue her higher education at the University of Bradford, UK. She is currently pursuing the PhD degree in the area operation and planning of distribution networks with penetration of renewable sources. Her main research interests include renewable energy, power system operation, control and optimization. She is a member of the Iraqi Engineering council since 1999.

Geev Mokryani is a Lecturer in electrical power systems at the Faculty of Engineering and Informatics, University of Bradford, UK. Prior to joining Bradford in February 2015, he was a postdoctoral research associate at Department of Electrical and Electronic Engineering, Imperial College London, U.K for two years. He received the BSc, MSc and PhD degrees in electrical engineering in 2004, 2007 and 2013 from Sahand University of Technology, Tabriz, Iran, and University of Salerno, Italy, respectively. He has authored three books, two book chapters and more than 50 research papers in top-class peer-reviewed international journals and conferences. He is associate editor of IET Generation, Transmission and Distribution and IET Renewable Power Generation and Wiley International Transactions on Electrical Energy Systems. He is Senior Member of IEEE and Fellow of Higher Education Academy. He is also a member of Member of CIGRE working group C1.40 and joint working groups C1/C4.36 and C1/C6/CIRED.37.